

PAPER • OPEN ACCESS

Performance assessment of direct injection compressed natural gas vehicle at different injection pressures using speed-sweep test method

To cite this article: M F A Rahim *et al* 2020 *IOP Conf. Ser.: Mater. Sci. Eng.* **788** 012068

View the [article online](#) for updates and enhancements.

Performance assessment of direct injection compressed natural gas vehicle at different injection pressures using speed-sweep test method

M F A Rahim^{1,2,*}, A A Jaafar², R Mamat³, Z Taha² and M H R Alias¹

¹ Automotive Engineering Research Group, Faculty of Mechanical & Automotive Engineering Technology, Universiti Malaysia Pahang

² Innovative Manufacturing, Mechatronics and Sport Laboratory, Faculty of Mechatronics & Manufacturing Engineering Technology, Universiti Malaysia Pahang

³ Advance Fluid Research Group, Faculty of Mechanical & Automotive Engineering Technology, Universiti Malaysia Pahang

*Corresponding email: mfadzil@ump.edu.my

Abstract. This paper presents an experimental study on a high-pressure direct injection compressed natural gas engine (HPDI-CNG) vehicle using speed-sweep test method. The objective of this work is to assess the performances of the HPDI-CNG after installation of a new DI configuration on the engine. The gas direct injectors which were converted from gasoline direct injection (GDI) unit injector are side-positioned on an inline 4-cylinder 4 stroke CAMPRO 1.6 engine with minimal cylinder head modification. The original electronic control unit was replaced with a programmable HALTEC controller and the engine was set to operate in bi-fuel mode. The HPDI-CNG vehicle prototype is tested on chassis dynamometer by using speed-sweep test procedure. The tests were carried out in vehicle simulation mode for acceleration from 20 mph to 40 mph based on the ramp input from idle-speed to wide-open throttle opening. The responses of the engine were recorded as transient output data. The HPDI-CNG engine output produced lower performances compared to the same engine with gasoline port injection. This is demonstrated by the maximum engine speed, brake torque and brake power which are recorded to be 2800 rpm, 63 Nm, and 17 kW respectively. It can be concluded that the use of side-positioned direct injector of HPDI-CNG system is unable to increase engine performance if compared to a gasoline port gasoline engine. Moreover, the use of throat- geometry has resulted in a lower performance of HPDI-CNG engine compared to a standard CNG-DI engine. The main factor which affected the HPDI-CNG engine is the ability of the system to deliver sufficient fuel mass at the correct amount and timing as well as the insufficiencies of the air supplies to oxidize the fuel completely.

Keywords. Alternative fuel, Direct-Injection, CNG, Vehicle Testing, Speed-sweep

1. Introduction

Nowadays, natural gas vehicles (NGV) are mostly based on the conversion of gasoline and diesel engine, performed by using CNG retrofit kit. Among critical parts in a compressed natural gas (CNG) fuel system are gaseous fuel dispenser, compressors and CNG storage cylinders (1). Nevertheless, it also requires gas pressure regulator/reducer, gas fuel filter, the ECU, MAP and speed sensor, gas piping and



gas fuel injectors/ mixer. Based on the converted CNG system, the NGVs can be divided into three categories, which are (a) dedicated NGV (b) bi-fuel NGV and finally (c) dual-fuel vehicle (2). Previous studies on port-injected CNG engines have suggested that the power loss of a CNG engine can be compensated by the use of direct injection CNG fuel system (3)(4). The adoptions of CNG-DI were also based on the conversion of existing spark ignition (SI) and compression ignition (CI) engine and most of the CNG direct injector were converted from gasoline direct injection (GDI) injector. As a result, the addition of GDI injector will require expensive and complicated modification of SI and CI engine cylinder head to accommodate the new injector.

The modification of cylinder head should be minimized especially for the modern, compact combustion chamber. In (GDI) engine, there are two basic charge modes; the stratified and homogeneous charge mixture mode. At the partial load conditions, stratified charge (late injection) is used, that is, fuel is injected during the compression stroke to supply the stratified charge. The engine can be operated at a very lean mixture and fully throttle-less operation is possible. On the other hand, a homogeneous charge (early injection) is preferred for the higher load conditions, that is, fuel is injected earlier during the intake stroke to provide a homogeneous mixture. (5). It is worth to highlight that; the common position of the direct injector's nozzles in a GDI engine is equally positioned with the surface of the combustion chamber wall. Hence, the gases exit the nozzle will instantly mix with the bulk amount of fresh air charge inside the combustion chamber to form a combustible mixture. This is a clear advantage of a GDI engine compared to the port fuel injection (PFI) gasoline engine. The mixture preparation time lag is shortened hence the response time of the engine's output torque due to throttle input changes shall be improved (6). Lake et. al (7) summarised that there are at least four configurations available to realize the direct injection engine configuration capable of producing acceptable combustion.

The available realizable concepts are 1) top entry ports with side injector 2) side entry port - side injector-swirl 3) side entry port – side injector-tumble, and finally 4) side entry ports with central plug and injector. Lake stressed out that the GDI system can be further tailored by advance technologies such as air-assisted injection, variable spray pattern systems, atomisation devices, injector pulsing strategy, and advanced control and ignition system technology. Kubesh (8) had explored a method to increase throttle-less CNG engine efficiency by created sufficient in-cylinder fuel-air charge. He utilised the direct injection stratified charge (DISC) and fuel injected pre-chamber (FIPC) methods. The FIPC combustion system was found to be a more practical solution to the problem of charge stratification. Huang (9) suggested that the parallel and single fuel injection produced a better mixture of stratification compared to the opposed injection. Both the parallel and single direct injection of natural gas able to operate in super lean condition due to the higher degree of stratification produced by both configurations. Cummins-Westport (10) had developed a natural gas engine capable of 2010 emission standards by the used of exhaust gas recirculation system (EGR), the spark assisted ignition and the three-way catalyst system for filtering the exhaust emission. Orbital Australia Pt. Ltd. (11) had developed a dedicated direct injection system for direct injection CNG engine in a 450cc single-cylinder research engine. It was found out that the engine performance was increased by up to 10% through the direct injection of natural gas without other modification on the engine. Boretti and Watson (12) had proposed a novel combustion system called a jet ignition device.

The system consisted of a centrally located DI injectors and a jet ignition (JI) device for combustion initiation of the main chamber (MC) mixture. The concept is resembling the indirect injection of CI engine however the system utilised two direct injectors. The use of two direct injectors and the installation of the jet ignition devices clearly limiting its applicability in actual cylinder head spaces. Another novel work related to the development of direct injection system for CNG fuel engine is the development of a spark plug fuel injector (SPFI) which is a combination of a fuel injector and a spark plug (13–15). The design of SPFI consists of a direct fuel injector which is combined with a spark plug using a specially fabricated bracket, connected to a fuel pipe and a fuel path running along the periphery of a spark plug body to deliver the injected fuel to the combustion chamber. Experimental results of the engine testing with SPFI shown that the volumetric efficiency is higher when compared to

port injection operation where the highest was achieved at 190° start of injection (SOI) timing. The highest fuel conversion efficiency, brake power and BMEP were also obtained at SOI of 190° BTDC. SPFI direct injection operation is found to be very sensitive towards injection timing and in agreement with the findings by (9) and (16). Aris et. al (17) had conducted an experimental study on two different piston crown types of CNG-DI engine namely the homogeneous and stratified combustion. It was found out that the start of injection (SOI) laid in between 120° BTDC to 180° BTDC had produced constant power and torque.

In order to accommodate the slower combustion duration, the ignition timing had been advanced to achieve a good performance where the default ignition timing is 18° BTDC and advanced to 24° BTDC to obtain the best results. The homogenous crown with a nearly flat surface produced a better torque compared to the stratified crown design. The maximum torque is 31.8 Nm at 3000 rpm, compared to 24.65 Nm for the stratified crown. The maximum power is 12.29 kW at 4000 rpm for homogeneous and 6.5 kW at 2500 rpm for the stratified crown. Kalam and Masjuki (4) conducted a study is to compare the results between CNG-DI, with CNG-BI and gasoline-PI engines with the same displacement volume. It was found that the CNG-DI engine produces similar brake power at 6000 rpm and wide-open throttle (WOT) but produces higher brake power at part load condition as compared to the original gasoline. The CNG-BI engine produces 23% lower brake power than the CNG-DI engine. The average brake specific fuel consumption (BSFC) of the CNG-DI engine was 0.28% and 8% lower than gasoline-PI and CNG-BI engines respectively. The CNG-DI engine reduces 42% NO_x emission as compared to the base engine. However, the CNG-DI engine produces higher HC and CO emissions as compared to the base engine.

A recent study of Moon (18) suggested that the CNG direct-injection also improved the engine performances in term of combustion speed, combustion stability and thermal efficiency especially at low-load conditions due to the action of spray induced turbulence at retarded injection timings. However, at high-load condition, the direct injection decreased the engine thermal efficiency and increased the hydrocarbon emissions due to the deteriorated mixture homogeneity. This indicates that by retarding the injection timing and forming a stratified charge mixture can produce better CNG-DI engine performance. Aljamali et. al (19) reported that high power, torque and brake mean effective pressure (BMEP) are obtained at end of injection (EOI) 120° BTDC. In addition, the lowest brake specific fuel consumption (BSFC) is also recorded at the same injection timing. The engine is operated at lean mixture condition. On emission, carbon monoxide (CO) emission is low at 360° BTDC at low speeds but at high speed, it was low at 120° BTDC. Carbon dioxide (CO₂) emission was high at 120° BTDC on the high engine speeds. The lowest (NO) and (HC) were founded at 120° BTDC at both lower and high engine rotational speed. They utilised injection pressure setup of 20 bar for all tested cases and a compression ratio of 14:1.

There are many recent reports published in the literature but most of the studies concentrated on the CNG engine improvement by the addition of hydrogen gases such as (20,21) or application of CNG in dual fuel engines (22,23). Both techniques required a more complicated fuelling system and are not readily available for commercial usage. Hence, this study will concentrate on the application of CNG for dedicated NGV or bi-fuel mode only which are expected to be more practical and affordable. Based on the discussion before, there were a few attempts to design and develop a dedicated CNG direct fuel injection system for spark ignition engine. The real reason for the innovation is due to the fact that the baseline engines (SI and CI) converted to CNG direct injection engine does not really accommodate the installation of the new direct injection system. This is true for a modern passenger vehicle engine which is compact in design. The modern combustion chamber of the spark ignition engines are mostly pent-roof designed. The space for the installation of the direct injector are very minimal and thus limiting the direct injector selection and alteration of injector position. Therefore, it can be concluded that, the design and development of direct injector configuration for CNG fuelling are still widely studied and researched.

A new configuration for a CNG-DI engine has been developed and tested, namely high-pressure direct injection of the compressed natural gas engine (HPDI-CNG) based on spark-ignition engine

platform. The injection pressure employed is higher than the setup in previous studies (which mostly utilized 20 bar of gas pressure) where currently the injection pressure setup is in the range of 45 bar to 60 bar. The new configuration utilized side injection with a throat like geometry or hollow passage which connected the combustion chamber with the injector nozzle. The injector itself is not mounted on the cylinder head body but firmly hold by an injector holder and injector bracket and disconnected with any engine bodies except through the throat passage. The purposes of such design are to minimize the cylinder head modification and overcoming the limited space available on the engine cylinder head. This paper reports an experimental engine testing conducted on the new engine configuration conducted with the objectives to assess the HPDI-CNG engine performances based on brake torque, brake power, brake thermal efficiency and brake specific fuel consumption. The second objective is to identify the operating envelope of the engine which is characterized by the engine MAP, engine rotational speed, ignition timing, injection duration and injection timing. These data are vital to benchmark as the baseline engine performances and for performances optimization in the next stage of the study.

2. Experimental Setup

2.1. Baseline prototype vehicle

Table 1 presents the technical specification of the baseline vehicle converted to compressed natural gas vehicle. The vehicle is made of Proton, model name Gen2, which is powered by 1.6 litres 4-cylinder inline spark-ignition engine namely S4PH CAMPRO. Each cylinder is designed with two intake and exhaust valves. The engine is powered by a multi-port injection (MPI) system. The top speed of the vehicle is 190 km/h whereas the maximum power is 82 kW at 6000 rpm. The maximum torque is produced at 4000 rpm with a value of 148 Nm.

Table 1. Specification of the baseline vehicle's engine for HPDI-CNG conversion.

Engine Specification	
Code	Proton S4PH CAMPRO
Type	In-line 4 cylinders, DOHC, 4 valves per cylinder
Bore/stroke	76/78 mm
Displacement	1597 cc
Compression ratio	10:1
Fuel delivery	Multipoint EFI
Fuel cut-off point	7000 rpm
ECU	Proton EMS700
Engine dimensions	581 mm (L) x 605 mm (H) x 650 mm(W)
Benchmarked Performance	
Top speed	190 km/h (Auto=185 km/h)
0 – 100 km/h	10.5 secs (Auto=13.0 secs)
Fuel consumption at constant 90 km/h	17.1 kms per litre/48.9 mpg (Auto= 15.9 kms, 45.5 mpg)
Max power	82 kW/110 bhp @ 6000 rpm
Max torque	148 Nm @ 4000 rpm

2.2. *Modification of the cylinder head*

One of the major concerns in this study is to minimize the modification made to the original engine configuration. The part under crucial consideration is the cylinder head of the engine. The main challenge for the new design of CNG-DI engine is the difficulty to provide sufficient space for the injector in the vicinity of the spark plug. As a result, the injector is located at the side location of the cylinder. Existing gasoline direct injection (GDI) engine mostly utilize tumble and squish motion strategy with central location injector. In order to accomplish this new CNG-DI engine, a new set of direct fuel injector for gases is installed into the engine. The location and numbers of the gasoline port fuel injectors are retained whereas an additional four direct injectors for CNG fuel are added. Figure 1 presents the engine, cylinder head and the installation location of the new CNG direct injectors which utilised a side-positioned cylindrical throat geometry that protrude into the cylinder head. Whereas the injector itself is fixed to the injector holder separated from the cylinder head body. Figure 2 presents a schematic of a cross-sectional view of the injector installation method. Based on this view, the direct injector for CNG was located just below the intake system of the engine.

2.3. *The CNG direct-injection system*

The CNG injection system has utilised four units of high capacity, GDI injectors made of Bosch to supply the gaseous fuel directly into the cylinder. The CNG and gasoline injectors are governed by the same electronic control unit (ECU), using the same base maps. Both injectors are of the different type where the gasoline port injectors are saturated type injectors and CNG direct injectors are peak and hold injectors. The maximum ECU current limit to the injectors is 8 Amp of saturated current. The saturated injector has high impedance and thus produce a much lower current compared to the peak and hold injectors.

The original Proton EMS700 ECU has been replaced with a new programmable ECU made of Haltech, model E8. The Haltech E8 ECU is used to control both the gasoline and gas injector, as well as the spark ignition unit. The key stage during the development of the HPDI-CNG is the tuning of the base maps. The crucial base maps here consist of the ignition timing maps, the injection duration maps and injection timing maps. The tuning process has been carried out in the first phase of the project where the vehicle ECU has been tuned by a team of professional tuners. It is important to highlight that the current study is executed with the assumption that the ECU base maps have been tuned to their best limit in the earlier phase of the project. And the tuning process was primarily conducted by the use of steady-state test on a chassis dynamometer. This is a widely practised, a traditional method of base maps tuning by using chassis dynamometer. Since the traditional tuning is a point-to-point “test and tune”, certain test points shall be left out and extrapolated in order to reduce the tuning cost. If we consider the operating point based on the size of the maps, the total points shall exceed $32 \times 32 = 1024$ points.

The CNG fuel storage system includes the storage tank, the tank pressure gauge, the delivery pressure gauge and regulator, the filling valve, the purge valve and supply shut off valve. The delivery pressure regulator is used to control the supply pressure of CNG gas to the injector’s common rail. The valve is manually regulated and thus becoming a true challenge to select the most appropriate pressure setup for the vehicle/engine. As up to this stage, by the combined use of the new direct fuel injection method and the pressure regulation, the combustion inside the engine only can be sustained at injection pressure setup of 45 bar – 60 bar. Beyond the stated range, the engine/vehicle output becoming highly sluggish and jerking. Therefore, throughout the study, the injection pressure setup of 45 bar, 50 bar, 55 bar and 60 bars were chosen to become the adjusted/controlled variables during the testing. The selected pressures setup are higher than 20 bars (which are mostly used by Malaysian NGV researchers) hence the new CNG-DI engine is called as high-pressure direct injection (HPDI) CNG engine to distinguish the new engine//vehicle against the previous work.

3. Experimental Procedures

The chassis dynamometer used in the study is a Mustang dynamometer, model MDK250 with inertia weight. This is the most important instrumentation throughout the study. The maximum absorbable horsepower of the dynamometer is 1500 hp/ 1118.55 kW with about 907.1847 kg of base mechanical inertia. Whereas the maximum rolling speed of the dynamometer is about 281.635 km/h. Figure 3 presents the layout of the chassis dynamometer and the data acquisition setup. The data from the dynamometer are measured and calculated continuously and the data resolution is fully adjustable. The interface of the dynamometer controller to the data-logging PC is made possible by the use of interface software named PowerDyne by Mustang.

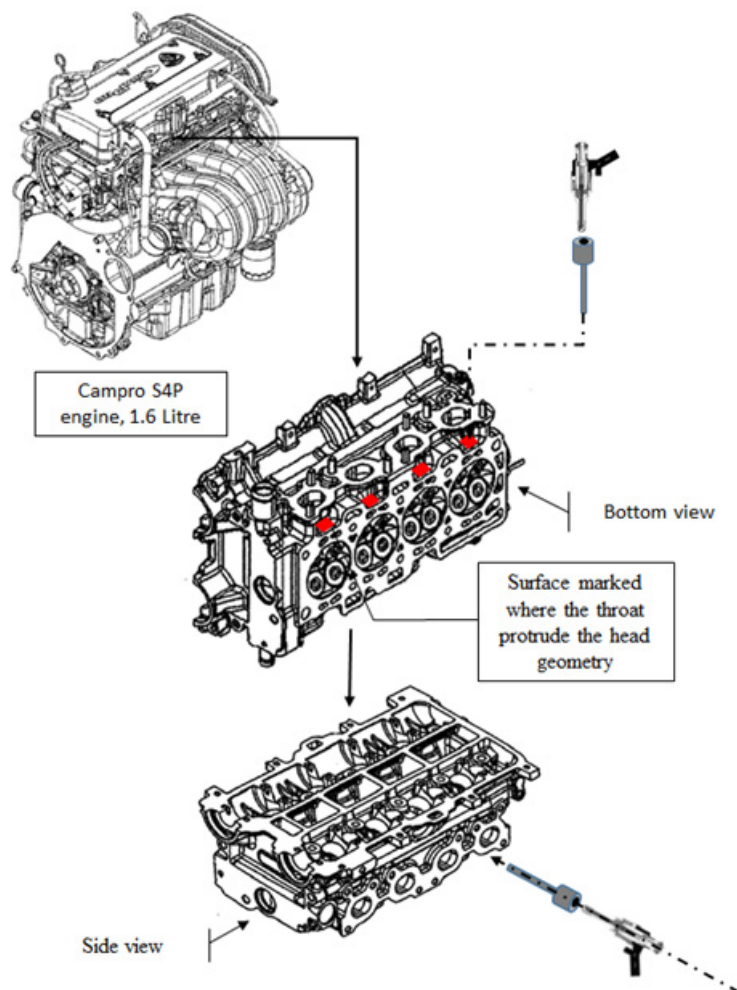


Figure 1. The engine, cylinder head and the installation location of the direct fuel injector.

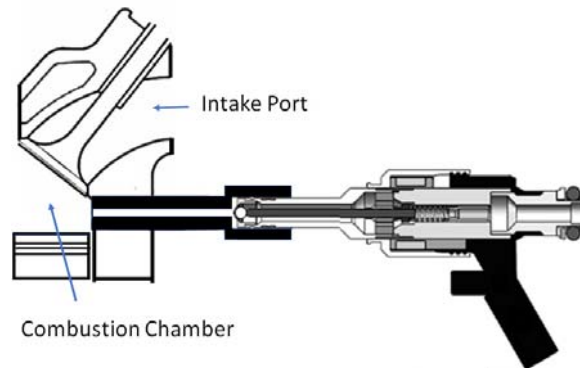


Figure 2. Schematic of a cross-sectional view of the injector installation method.

The throttle and intake manifold system of the engine is connected to a surge tank which equipped with a laminar flow element. This laminar flow element (LFE) is originally used to measure the mass flow rate of the air intake by using differential pressure approach. However, it was found out that the usage of the LFE has resulted with over restriction of the air intake and thus lowering the maximum engine torque and power especially when the test was carried out at wide-open throttle condition and high engine speed. Instead of this, the intake airflow can also be estimated by the use of manifold absolute pressure data with the speed-density method. The instantaneous ECU parameters can be monitored and logged by the use of interface software named Halwin. Almost 20 parameters were monitored and logged from the ECU in each test. Among the parameters are engine speed, injection duration, ignition timing, injection timing, injector duty cycle, coolant temperature, air intake temperature, throttle position, intake air manifold absolute pressure, correction factors and others. The ECU parameters are highly important since our current study intended to analyse the effect of all the ECU parameters on the vehicle/engine output performance. The AFR data is measured based on the exhaust gas analysis. The Innovate air-fuel ratio meter has been used for every test executed. The location of the oxygen sensor is just after the exhaust port of the engine. The sampling of the exhaust gas is made just before the three-way catalytic converter of the engine to ensure the accuracy of the air to fuel ratio which taken to be representative of the mixture formed in the combustion chamber.

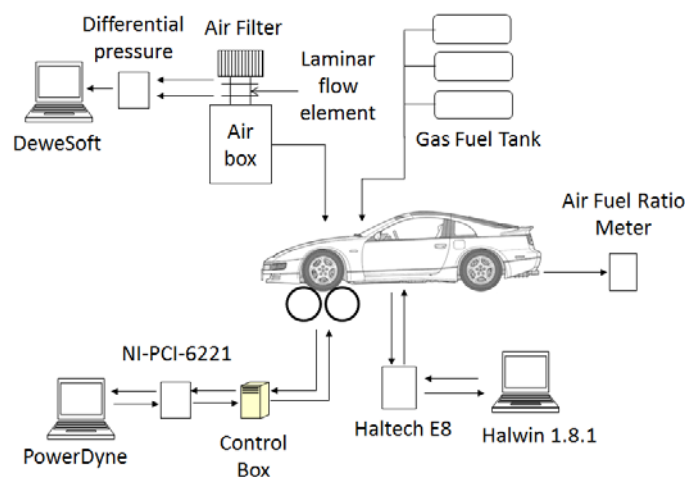


Figure 3. Experimental layout for speed-sweep chassis dynamometer test and schematic of data acquisition system layout.

3.1. Speed-sweep test method

In order to measure the power and torque of the CNG-DI vehicle, chassis dynamometer testing of the vehicle has been carried out. There are three basic types of test allowable using chassis dynamometer which are the steady-state test, sweep test and transient test. The steady-state test is done by fixing engine speed at a specific engine revolution and other variables such as dynamometer load at a fixed value as well. Under sweep test, the test vehicle is loaded with constant inertia load only (without current-induced load), but the engine is allowed to sweep from starting speed until final stopping speed. Whereas under transient test, both the engine speed and load are varying with time [24]. Most of the transient test application is related to an emission measurement standard. Some of the criteria of transient test including aggressive throttle movements, engine speed changes, and engine motoring. In the current study, instead of generating performance data of the engine, the study also intended to minimize the number of operating test point. Therefore, speed-sweep test procedure has been selected as the test method. This method offers a very significant advantage over other test methods since the torque-curve or the power-curve can be produced instantly. The engine speed is allowed to sweep across the operating range of the engine. If the engine is operated at its wide-open throttle condition, the maximum power/torque curve of the engine shall be obtained. The speed-sweep test method requires some information on the tested vehicle such as the vehicle mass and the engine power at 50 mph. The vehicle-simulation-loading mode will most accurately reflect the actual power that the vehicle will deliver in use [24]. The test was executed by providing a ramp input to the driver pedal continuously until the test stopped. The start and stopped test criteria used are the minimum and maximum lateral vehicle speed which are equal to 25 mph to 40 mph. The selection of the values is made based on the lateral speed range of the vehicle examined prior to the actual test. The maximum throttle opening tested is 100% (wide-open throttle). The power and torque were corrected based on SAEJ1349 standard.

4. Results and discussion

4.1. Engine input parameters

The results of the speed-sweep test are broadly categorized as the engine input and engine output parameters. Parameters which are classified as engine input are throttle position sensor, manifold absolute pressure (MAP), injection timing, injection duration, ignition timing and air to fuel ratio. All data are tested at 45, 50, 55 and 60 bar injection pressure. Two sets of data of each injection pressure setup are presented in this paper.

4.1.1. Manifold Absolute Pressure (MAP). The manifold absolute pressure (MAP) variation is presented in Figure 4. The absolute pressure is strongly correlated with the throttle angle opening. As the throttle angle opening is increased to 100% opening, the MAP value inside the manifold is increased (became positive) and approaching the surrounding ambient pressure (0 kPa abs). The highest pressure recorded during the testing is 4 kPa, which is the highest possible MAP can be sensed by the MAP's sensor. As the speed swept through the test window, and the MAP is constant at about 0-4 kPa, all other parameters are changed accordingly. The most obvious is the gradual increment of engine rotational speed. This is because, MAP value, (together with engine rotational speed) are independent parameters utilised by the ECU to determine the instantaneous operating point of the engine (axis of the look-up tables/ map). Therefore, any increment in MAP will affect other parameters too especially the output parameter. The recorded MAP after the 100% opening, which is in the range 0 - 4 kPa (abs) is consistent with the characteristics of a naturally aspirated induction system of the engine. The MAP reading almost consistent until the end of the test because the throttle is held at wide-open condition until the end of the test.

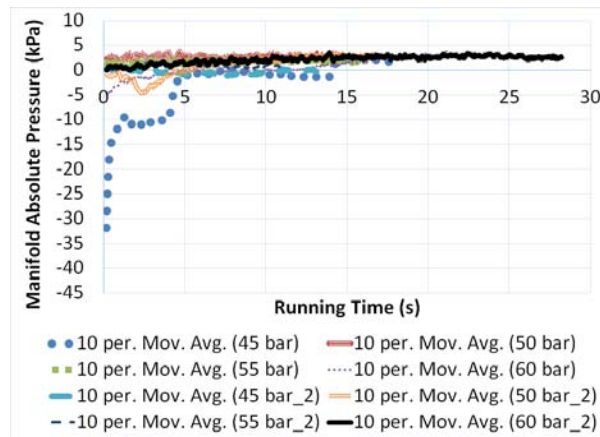


Figure 4. Manifold absolute pressure for the speed-sweep test at different injection pressures.

4.1.2. Injection timing. The injection timing parameter is represented by the end of injection (EOI) in relative to top dead centre during the firing stroke. Based on the presented results by figure 5, as the throttle opening was increased, the injection timing was advanced further in relative to top dead centre. Overall, the most advanced and retarded injection timing is about 5000 CA and 4730 CA before top dead centre (BTDC) respectively. The value of EOI proportionally changes with engine rotational speed. This is because the injection timing was set as a function of engine speed within the ECU setup. Hence, as the engine rotational speed is increased, the injection timing is advanced. The increment of the EOI will follow closely the path and rate of the engine rotational speed increment. The EOI needed to be advanced because, as the speed increased, the cycle period is becoming shorter, where the mixing time for air and fuel mixture has also been shortened, thus the EOI must be made quickly before the spark firing closed to the TDC. A different path of the injection timing variations is plotted by the different injection pressure setup because each injection pressure setup produced a different path for engine rotational speed increment. In greater details, each injection pressure had produced different nett torque and consequently produced different engine rotational speed.

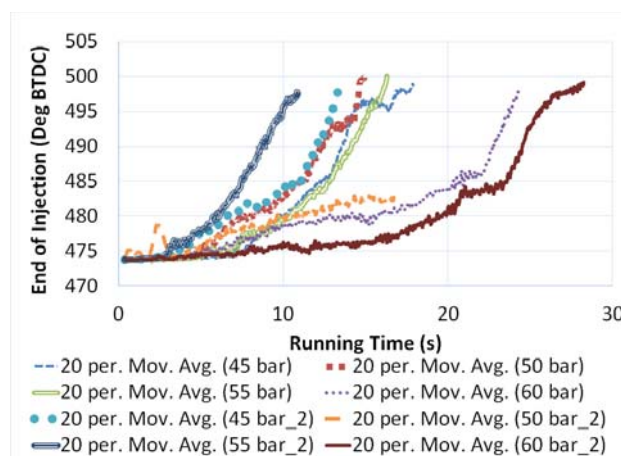


Figure 5. Injection timing for the speed-sweep test at different injection pressures.

4.1.3. Injection duration. Figure 6 presents a plot of injection duration for the HPDI-CNG vehicle at different injection pressure. The injection duration values are predefined in the ECU maps and it was set up as a function of engine rotational speed and MAP. Based on the plotted graph, the maximum and minimum values are about 20 ms and 11 ms respectively but most of the data are concentrated within 16 ms to 20 ms. As the engine rotational speed and MAP are increased, the injection durations are increased but the increment is limited to 20 ms. These are equivalent to 93% duty cycle of the injector. This could be an inter-related effect between the injection duration and engine rotational speed. The maximum engine speed recorded during the test was only 2900 rpm and at the same time, the duty cycle of the injector was already met 93%, which probably limiting the fuel supplied to the engine cylinder. To further increase the torque, more fuel is required but the injector had nearly met the maximum duty cycle. Therefore, the injection duration had limited the maximum engine torque and engine rotational speed. The slightly fluctuated injection durations have resulted from slightly fluctuated engine rotational speed. The injection pressure setup is not affecting the injection duration except more fuel is delivered at a higher pressure for specific injection duration.

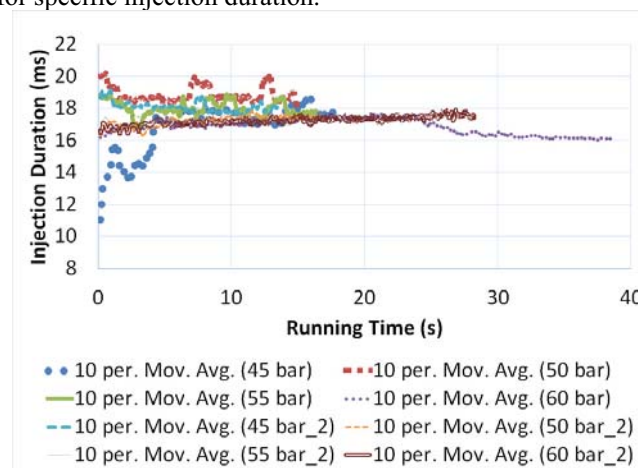


Figure 6. Corrected injection duration of HPDI-CNG vehicle for the speed-sweep test at different injection pressures.

4.1.4. Ignition timing. Figure 7 presents the ignition timing for HPDI-CNG engine at different injection pressure. The value of ignition timing is predefined in ECU maps. Based on the graph, the ignition timing is advanced as the engine rotational speed and MAP are increased. The maximum and minimum ignition timing advanced are about 23 BTDC and 12 degrees BTDC respectively. The path of ignition timing increment and its values have followed the path of the engine rotational speed and MAP of the engine. Since the resultant engine rotational speed at each injection pressure setup is increased at different rates, the ignition timing had also changed at different rates. Practically, when the speed and load increase, the ignition timing will advance to facilitate the faster combustion period. It is vital to achieve the peak combustion pressure at about 10 degrees after top dead centre in order to transfer the maximum work to the piston. This is called the maximum brake torque timing (MBT). In the current study, it is assumed that the best values of ignition timing at each operating point has been defined through the base map tuning process in the earlier phase of the study. Attempt to adjust the values beyond the prior selection mostly end up with sluggish engine operation and power loss. Nevertheless, this test let us know the tuned timing at the tested points.

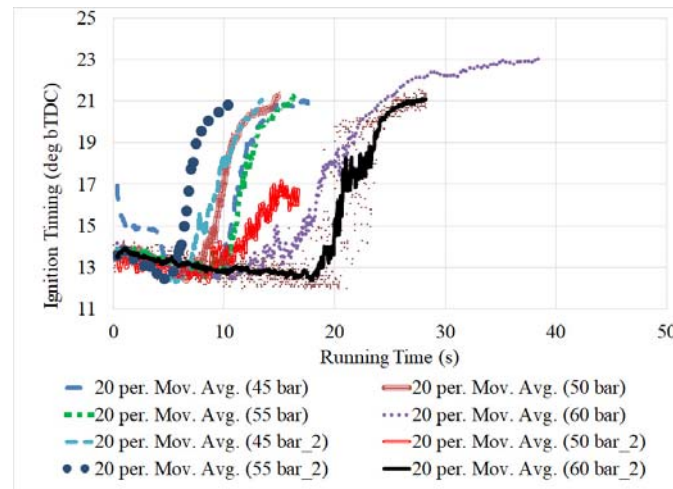


Figure 7. Corrected ignition timing of HPDI-CNG vehicle for the speed-sweep test at different injection pressures.

4.1.5. Air to Fuel Ratio (AFR). Figure 8 presents the resultant air to fuel ratio (AFR) of HPDI-CNG engine at different injection pressure. The stoichiometric AFR for CNG fuel is about 17. Thus, the overall AFR values recorded during the test were on the rich side. Based on the plot of air to fuel ratio against the test time, the leanest mixture's AFR is produced by the injection pressure of 45 bar at a value of 15.7. And the richest mixture's AFR is produced at an injection pressure of 60 bar with a value of 10.4. As the injection pressure is increased from 45 bar to 60 bar, the mixture produced by the engine is increasingly richer. The air to fuel ratio is highly affected by the injection pressure and injection duration because both parameters affecting the fuel supplied to the cylinder. Furthermore, both parameters are affected by engine rotational speed and MAP. The resultant AFR recorded fall in the rich side because it is common to set up the mixture richer at wide open throttle operation. Theoretically, at increase engine speed and load, the ECU will intend to provide a richer mixture to the engine in order to produce more torque and power. This is noticeable within the plot where the trend of the air to fuel mixture plot showing a slightly increasing trend from the test startup until the end of test time for the most injection pressure setup.

In most of the results, all the measured input data clearly highlight the fluctuation condition from the start until the end of the test. The input data to the engine are produced by the ECU based on the load requirement by the vehicle driver (where in this test, the vehicle was in accelerating condition). The reason for the fluctuated conditions is due to the ECU which continuously referring to the engine rotational speed as its input to read the lookup table (the resultant engine rotational speed is fed back to the ECU as the input). When torque and consequently the engine rotational speed have fluctuated, the ECU produced a fluctuated output as well. The origin of the fluctuation is the fluctuated AFR. This fluctuation had created a major impact on the resultant torque and consequently on the engine rotational speed. Since the injection pressure is constant and manually controlled, the fluctuation of injection duration is believed to contribute to the fluctuation of AFR. Other factors that possibly contributed to the current results are the time lag or delay in fuel delivery existed during the fuel travelling from exit of injector nozzle to the combustion chamber volume. This time lag has resulted in improper combustion controlled and possibly created high unburnt fuel to the exhaust and limiting the engine power and torque.

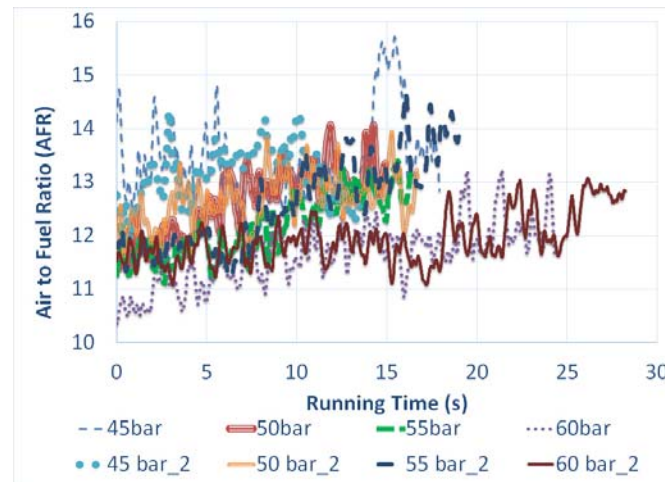


Figure 8. Air to fuel ratio of HPDI-CNG vehicle for the speed-sweep test at different injection pressures.

4.2. Engine output parameter

Parameters which are classified as engine output parameters are engine speed, engine total brake torque and total brake power, engine thermal efficiency and brake specific fuel consumption.

4.2.1. Engine speed. Figure 9 presents the plot of engine rotational speed in rpm against test time for different injection pressure. In all tests, the set start speed is referring to a lateral vehicle speed of 25 km/h while the end test speed was set to 40 km/h. Both minimum and maximum engine rotational speed in figure 9 are coincident with the starting and stopping speed criteria. The maximum lateral vehicle speed of 40km/h is selected as the stopping criteria since it is the maximum lateral speed achievable by the vehicle is most injection pressure setup. Based on the results presented in the graph, the engine rotational speeds started to increase as the throttle is pushed to the maximum throttle opening. For all cases, the vehicle achieved the lateral speed of 40 km/h at 2800 rpm of engine rotational speed since all the test were carried out at the same gear ratio. The only differences between the graphs are the time required to achieve the test stopping speed at 40 km/h. There are at least two main explanation for the results. First, the test was carried out at a slightly different throttle angle opening rate. Second, which is more important, different injection pressure setup which are used produced a different amount of fuel and mixture AFR. Based on the plotted graph, the injection pressure setup which managed to achieve the maximum stop speed in the shortest time is the low injection pressure setup at 45-50 bar. Whereas the injection pressure of 60 bar possessed the longest time required to achieve the maximum vehicle speed. This is because the lowest injection pressure setup produced the highest torque compare to the high injection pressure setup. This has generated a higher acceleration capability. Whereas, at an injection pressure setup of 60 bar, the generated torque is lower hence the vehicle produced a lower acceleration and acquired a longer time to achieve the maximum speed. In further details, the reason for the lower injection pressure setup to produced higher torque is due to a more complete combustion occurred at that pressure setup thus allowing a higher conversion of useful work compared to the higher injection pressure setup. There is a possibility that, at the higher injection pressure setup, more fuel is wasted and is not convertible to produce useful work by the engine.

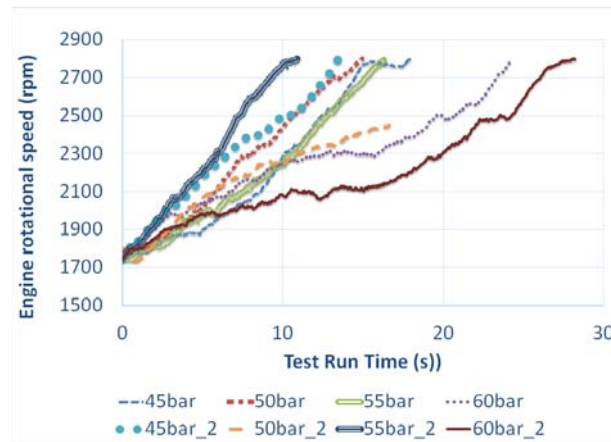


Figure 9. Engine speed of HPDI-CNG vehicle at different injection pressures

4.2.2. Torque and power. Figure 10 presents the engine output of the total brake torque of HPDI-CNG vehicle at different injection pressure. Based on the graph, the total brake torque showing a highly fluctuated trend without any significant increment or decrement in the mean torque value at each injection pressure. The fluctuation of total brake torque is produced due to the fluctuation of the AFR. A quite significant difference is noticeable between total brake torque magnitudes for each injection pressure. The highest torque produced by the use of low injection pressure setup. Whereas the lowest total brake torque produced by the use of the highest injection pressure setup. The maximum brake torque produced is about 63 Nm at 45 bar and the lowest total brake torque produced is 25 Nm at 60 bar. As stated before, we expect that the combustion at the low injection pressure setup produced more complete combustion thus allowing conversion of higher useful torque at the crankshaft. Figure 11 presents the total brake power produced by HPDI-CNG vehicle for different injection pressure. Unlike the total brake torque, the total brake power demonstrates a slight increment throughout the test time for each injection pressure. The brake power is a product of engine brake torque and engine speed. After the test commenced, the vehicle/engine speed is increased gradually until maximum speed. Thus, the resultant brake power increase as well throughout the test time. The magnitude of total brake power fluctuated throughout the test time. This is because the magnitude of brake power is calculated based on the torque. Therefore, the fluctuation is indeed inherited from the torque characteristics. The used of 45 bar injection pressure has produced the highest brake power which is about 17 kW during the test. The lowest brake power of about 6 kW is produced by the used of maximum injection pressure, 60 bar. The conversion of chemical energy towards mechanical work of torque is expected to be more successful at lower injection pressure setup due to more complete combustion occurred at that pressure setup. Even though, a higher amount of fuel supplied at higher injection pressure, the fuel might be wasted, not fully convertible to useful torque which is primarily due to the insufficient oxidizer when the mixture is too rich or the inability of the engine to induce sufficient air into the cylinder. The results of the total brake power and torque recorded in the current study are higher than the reported results by Aris et. al (17).

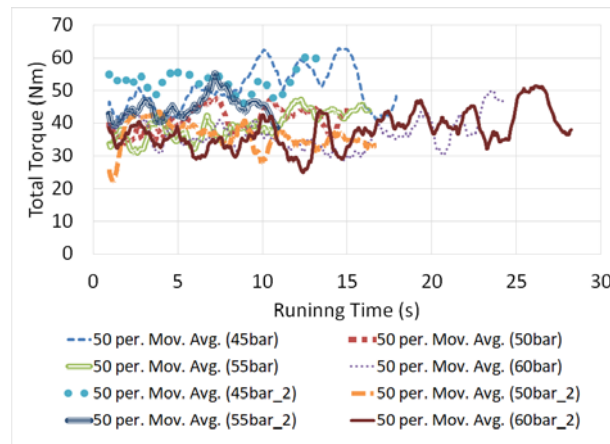


Figure 10. Engine total brake torque of HPDI-CNG vehicle for the speed-sweep test at different injection pressures.

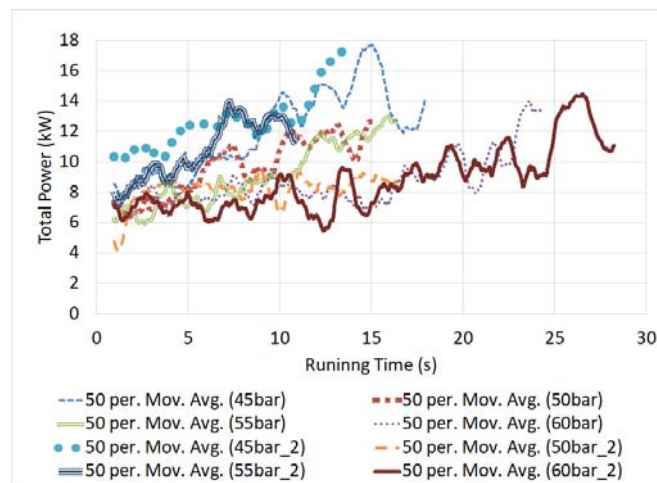


Figure 11. Engine total brake power of HPDI-CNG vehicle for the speed-sweep test at different injection pressures.

4.2.3. *Brake Thermal Efficiency (BTE)*. Figure 12 presents the brake thermal efficiency (BTE) of HPDI-CNG vehicle calculated at different injection pressure. Brake thermal efficiency is the ratio of the engine output power to the input energy supplied (mass flow rate x heating value) to the vehicle. Based on the plot, the thermal efficiency of the HPDI-CNG vehicle is slightly increased when the speed swept along the test time. The slight increment of the BTE is influenced by the increment of total brake power when the engine rotational speed increased. The thermal efficiency at each injection pressure shows a significant difference in terms of magnitude. The highest thermal efficiency trend is obtained with the use of the lowest injection pressure at 45 bar with a value of about 45 %. And the lowest thermal efficiency is obtained at the highest injection pressure of 60 bar with a value of 11%. This indicates that the vehicle is more efficiently operated at an injection pressure of 45 bar. Even though at this injection pressure the supplied fuel is lower than high injection pressure, but the conversion efficiency of mechanical work is higher due to a more suitable AFR ratio to produce higher torque. At high injection pressure, when the conversion is done at lower efficiency, more fuel is wasted. This is might be due to

insufficient air intake or excess of fuel supplied to each cylinder. Higher thermal efficiency is desirable since it indicates a higher amount of power produced by a unit amount of fuel.

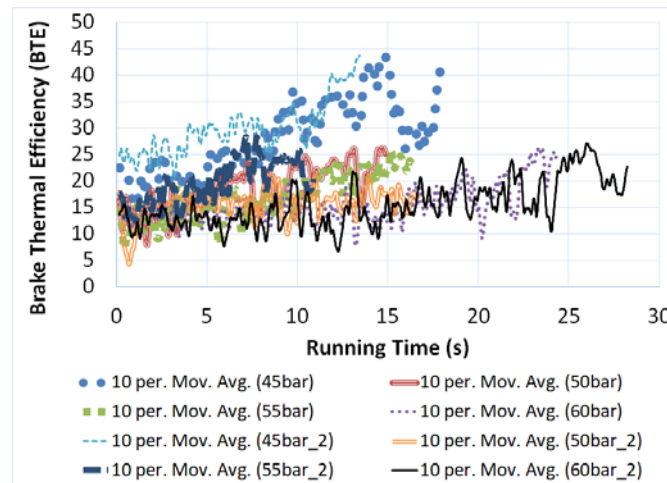


Figure 12. Brake thermal efficiency of HPDI-CNG vehicle at different injection pressures.

4.2.4. Brake Specific Fuel Consumption (BSFC). The brake specific fuel consumption, BSFC is the ratio of the fuel mass flow rate to the total brake power of the engine. Figure 13 presents the variation of BSFC during the speed sweep test procedure for different injection pressure. Based on the graph, at all injection pressure, the BSFC plots showing a decreased trend as the time progressed. The decreasing of BSFC is preferable as it indicates a reduction in fuel consumption. This can be explained by the fact that, as the engine speed and load are increased, the engine utilises a lesser amount of fuel to accelerate the vehicle. At the start of the test, more fuel is used to overcome the inertia load of the dynamometer and the vehicle body. The BSFC plots shown significant different magnitude at different injection pressure. The lowest injection pressure of 45 bar produced the lowest BSFC. And the highest BSFC is produced by the highest injection pressure of 60 bar. This indicates that the use of the lowest injection pressure at 45 bar utilised the lowest amount of fuel to generate a unit kW of power. The maximum BSFC measured from the test is about 780 g/kWh at an injection pressure of 60 bar and the lowest recorded is about 180 g/kWh at an injection pressure of 45 bar. It seems that the used of 45 bar injection pressure is sufficient, however, this can be further discussed due to the fact that, at higher engine rotational speed and load, more amount of fuel is needed to generate higher engine torque (which only can be provided by the use of higher fuel injection pressure). In addition, the produced brake torque and power produced so far is at a moderate level. Again, as we stated before, this might be the results of insufficient fresh air intake to oxidize the supplied fuel. The utilised intake system and the direct fuel injector is a standard unit without any major modification made on their physical state, therefore, it is expected that the air supplied is sufficient as in common port injected engine.

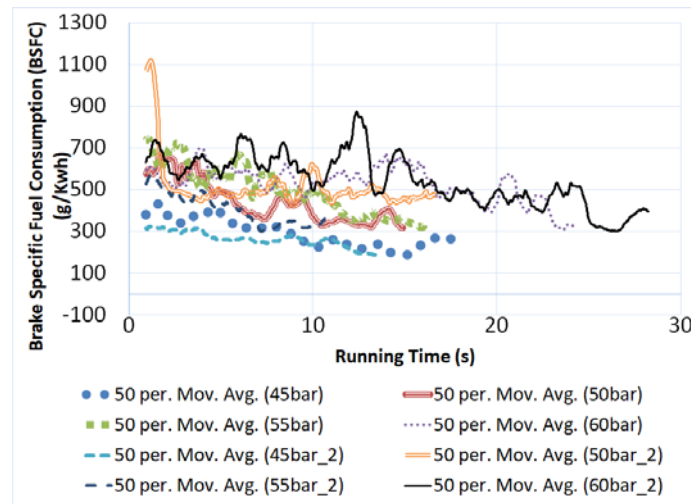


Figure 13. Brake specific fuel consumption of HPDI-CNG vehicle at different injection pressures

Investigation on the valve timing diagram as shown in figure 14 indicates that the EOI completed during/within the exhaust stroke (where the start of injection (SOI) might commenced during the exhaust or power stroke). As a result, by the beginning of intake stroke, the in-cylinder pressure, which is already high, is becoming higher due to mass transfer of CNG gases into the cylinder. Even though in the successive process, the piston is moving downwards (the volume expanded) and the in-cylinder pressure is becoming lower, there is a possibility that the in-cylinder pressure is still greater than the manifold pressure. Hence, this will end up with reduced suction capabilities and consequently lowering the volumetric efficiency of the engine. This is the reason why the amount of air is insufficient to fully oxidize the fuel. A probable solution to increase air intake is to boost the intake process.

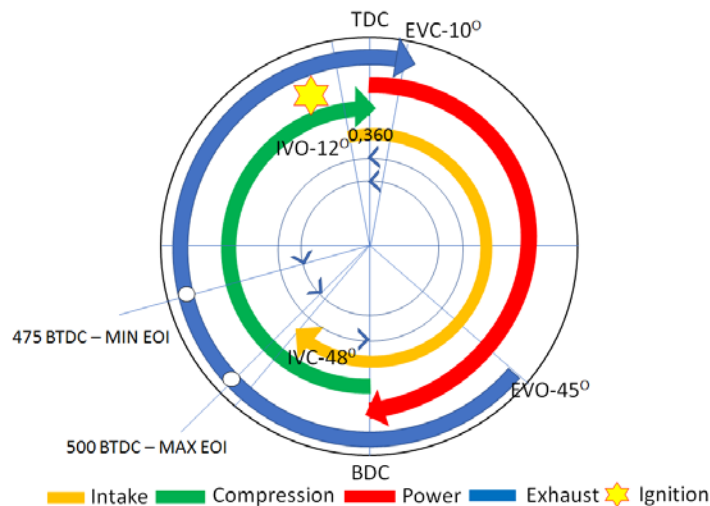


Figure 14. The valves timing diagram for HPDI-CNG engine and the location for minimum and maximum EOI.

5. Conclusions

The HPDI-CNG vehicle performance testing was carried out in order to assess the HPDI-CNG engine performance and to identify the operation envelope of the engine. Based on the results, the following summaries can be highlighted. The tests had been carried out at the engine maximum operable range (at wide-open throttle) condition. Therefore, the results are expected to represent maximum HPDI-CNG engine performances. The minimum and maximum manifold absolute pressure are -32 KPa and -4 kPa respectively. The most advanced and the most retarded injection timing are 500⁰ CA BTDC and 475⁰ CA BTDC respectively. The shortest and the longest ignition duration are about 11 ms and 22 ms respectively. The most advanced and the most retarded ignition timing advances are about 23⁰ BTDC and 12⁰ BTDC respectively. And finally, the air to fuel ratios have fluctuated in the range of 15.7 and 10.4. These data explain the operating envelope of the HPDI-CNG engine during vehicle testing. In general, the HPDI-CNG engine output produced lower performances compared to the same engine with gasoline port injection version. This is demonstrated by the maximum engine speed, brake torque and brake power which are recorded as 2800 rpm, 63 Nm, and 17 kW respectively. The maximum brake torque is less than half of 148 Nm which is the maximum brake torque of gasoline port injection version of the baseline engine. The maximum engine speed of HPDI-CNG is also less than half of maximum engine speed for gasoline port-injection version which is about 7000 rpm. It can be concluded that the use of side-positioned throat geometry HPDI-CNG system is unable to increase engine performance if compared to a port-injected gasoline engine. Moreover, the use of throat geometry has resulted in a lower performance of HPDI-CNG engine compared to a standard CNG-DI engine. The total brake power and torque are limited by the ability of the injector to supply the amount of fuel required by the engine. Even though at high injection pressure, the amount of fuel is increased, this also couldn't be benefited by the engine as the amount of air induced by the engine is restricted by the excess pressure inside the engine cylinder. The fluctuated engine performances in all parameters are resulted by the lag in fuel flow and poor response by the engine causing combustion instability.

Acknowledgements

We would like to express our sincere gratitude to The Ministry of Education and Universiti Malaysia Pahang who has funded the study under research grant numbered FRGS/1/2017/TK03/UMP/03/2 and RDU1703145, members of Automotive Laboratory, Innovative Manufacturing, Mechatronics and Sports laboratory, and Faculty of Mechanical and Automotive Engineering Technology which facilitate the study from the beginning.

References

- [1] Yeh S. 2007 An empirical analysis of the adoption of alternative fuel vehicles: The case of natural gas vehicles. *Energy Policy* **35** 11 5865–75.
- [2] Khan MI, Yasmin T, Shakoor A. 2015 Technical overview of compressed natural gas (CNG) as a transportation fuel. *Renew Sustain Energy* **51** 785–97.
- [3] Sementa P, Maria Vaglieco B, Catapano F. 2012 Thermodynamic and optical characterizations of a high-performance GDI engine operating in homogeneous and stratified charge mixture conditions fueled with gasoline and bio-ethanol *Fuel* **96** 204–19
- [4] Kalam MA, Masjuki HH. 2011 An experimental investigation of a high-performance natural gas engine with direct injection. *Energy* **36** 5 3563–71
- [5] Binder A, Ecker R, Glaser A, Müller K. 2015 Gasoline direct injection. In: Reif K. (eds), editor. *Gasoline Engine Management Bosch Prof.* Wiesbaden: Springer Fachmedien Wiesbaden, p. 110–21.
- [6] Zhao F, Lai M, Harrington DL. 1999 Automotive spark-ignited direct-injection gasoline engines *Prog Energy Combust Sci* **25** 437–562
- [7] Lake TH, Stokes J, Whitaker PA, Crump J V. 1998 Comparison of Direct Injection Gasoline Combustion Systems. *SAE Technical Paper Series*

- [8] Kubesh JT. 2001 Development of a Throttleless Natural Gas Engine. *SAE Tech.* **724**
- [9] Huang Z, Shiga S, Ueda T, Nakamura H, Ishima T, Obokata T, et al. 2003 Basic characteristics of direct injection combustion fuelled with compressed natural gas and gasoline using a rapid compression machine. *Proc Inst Mech Eng Part D J Automob Eng* **217** 11 1031–8.
- [10] Kamel MM. 2005. Development of a Cummins ISL Natural Gas Engine at 0.2 g/bhp-hr. Cummins Westport Vancouver, British Columbia, Canada.
- [11] Caley D, Cathcart G. 2012 Development of a natural gas spark ignited direct injection combustion system. NGV2006, Cairo, Egypt; 2006
- [12] Boretti AA, Watson HC. 2009 The lean burn direct injection jet ignition gas engine. *Int J Hydrogen Energy* **34** 18 7835–41
- [13] Iskandar T. 2010 Compressed Natural Gas Direct Injection (Spark Plug Fuel Injector). Natural Gas. Ch. 13.
- [14] Mohamad TI, Geok HH. 2008 PLIF Flow Visualization of Methane Gas Jet from Spark Plug Fuel Injector in a Direct Injection Spark Ignition Engine. Proceedings of the 1st WSEAS International Conference on VISUALIZATION, IMAGING and SIMULATION 35–40.
- [15] Mohamad T, Harrison M, Jermy M, Heoy Geok H. 2010 The structure of the high-pressure gas jet from a spark plug fuel injector for direct fuel injection. *Journal of Visualization* **13** 121–131
- [16] Zeng K, Huang Z, Liu B, Liu L, Jiang D, Ren Y, et al. 2006 Combustion characteristics of a direct-injection natural gas engine under various fuel injection timings. *Appl Therm Eng.* **26** 806–13
- [17] Aris I, Zainuddin KN, Alina NA, 2009 Torque and Power of CNGDI Engine with Two Different Piston Crown Shapes. *J Appl Sci Res* **5** 8 949–54.
- [18] Moon S. 2018 Potential of direct-injection for the improvement of homogeneous-charge combustion in spark-ignition natural gas engines. *Appl Therm Eng.* **136** 41–8
- [19] Aljamali S, Abdullah S, Wan Mahmood WMF, Ali Y. 2016 Effect of fuel injection timings on performance and emissions of stratified combustion CNGDI engine. *Appl Therm Eng* **109** 619–29
- [20] Hora TS, Agarwal AK. 2016 Effect of varying compression ratio on combustion, performance, and emissions of a hydrogen-enriched compressed natural gas-fuelled engine. *J Nat Gas Sci Eng* **31** 819–28
- [21] Bhasker JP, Porpatham E. 2017 Effects of compression ratio and hydrogen addition on lean combustion characteristics and emission formation in a Compressed Natural Gas fuelled spark ignition engine. *Fuel* **208** 260–70
- [22] Singh E, Morganti K, Dibble R. 2019 Dual-fuel operation of gasoline and natural gas in a turbocharged engine. *Fuel* **237** 694–706.
- [23] Ouchikh S, Lounici MS, Tarabet L, Loubar K, Tazerout M. 2019 Effect of natural gas enrichment with hydrogen on combustion characteristics of a dual fuel diesel engine. *Int J Hydrogen Energy* **44** **26** 13974–87
- [24] Mustang 2005 Mustang Dynamometer -Power Dyne PC Operators Manual. Twinsburg, Ohio: Mustang Dynamometer